1.5kW LLC Resonant Converter with improved interleaved winding structure and core structure

Yuhang Xu[1], Xu Yang[1], Jiwen Wei[1], Suchen Dong[1], Wenjie Chen[1] and Kangping Wang[1]
[1] Xi'an Jiaotong University, China

***Abstract*-- In recent years, the power supply of the data center is increasing day by day. The new power supply architecture uses 48V bus to supply power to the subsequent VRM, so as to reduce I2R loss. Because of its soft switching characteristics, LLC resonant converter can meet the requirements of high power density and high efficiency, and is used in isolated DC−DC converter. In this paper, a magnetic integrated transformer is proposed to reduce winding loss and core loss. The windings and magnetic cores are optimized in local detail. A 1500W module was made in the experiment, achieving 97.8% peak efficiency and 97.6% efficiency at full load.**

***Index Terms*-- Matrix transformer; magnetic integration; terminal loss Introduction**

I. INTRODUCTION

With the increase of power supply in the data center, there is a higher requirement for the efficiency and power density of power electronic devices. The 48V bus architecture has two advantages over the current 12V architecture[1]. (1) Reduce the condution loss of secondary winding so as to achieve low transformer loss. (2) The 48V bus architecture can be equipped with 16S batteries, saving the UPS part of the 12V architecture. Therefore, the 48V bus structure has been widely used.

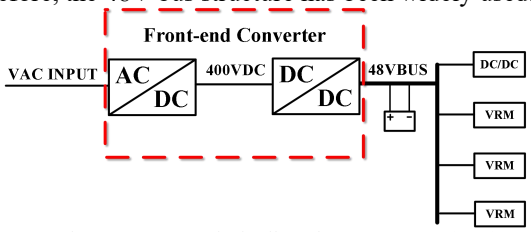

Fig. 1. Structure of Distributed Power System(48V)

On the other hand, LLC resonant converters can achieve high efficiency and high power density, which can achieve zero-voltage switching (ZVS) for the high-side switches, and zero-current switching (ZCS) for the SRs. So it has been widely used server, telecom application and on board charger (OBC)[2]-[4].

In power electronic devices, magnetic component loss accounts for more than 50% of the total loss. And DCX mode for LLC resonant converter has high efficiency and large inductance ratio. Leakage inductance of transformer can be used as resonant inductance. The optimization of transformer loss becomes very important.

For the traditional transformer, it needs to occupy more PCB layers for excessive current, and the secondary side needs multiple tubes for parallel connection, so large terminal loss will be generated at the connection. The matrix transformer can reduce the core size and core loss through magnetic flux cancellation, and can reasonably parallel the secondary current to reduce the winding loss[5]. CPES proposed a magnetic integrated core structure, which integrates the resonant inductor and transformer into one magnetic core[6]. In the lower frequency DCX mode, the leakage inductance of the transformer is not enough to meet the value of the resonant inductance, so two center columns are added. This paper uses a magnetic core structure, which combines two magnetic poles together to increase Ae, so the required resonant inductance can be achieved with low turns.

This paper focused on the staggered structure of winding and the optimization design of magnetic core structure, and compares the loss and loss distribution under different schemes, which provides the optimization design of magnetic parts. The winding structure is also fully staggered, so that the magnetomotive force between the primary and secondary sides is evenly distributed, and the leakage inductance and AC impedance are reduced.

II. LLC TRANSFORMER DESIGN

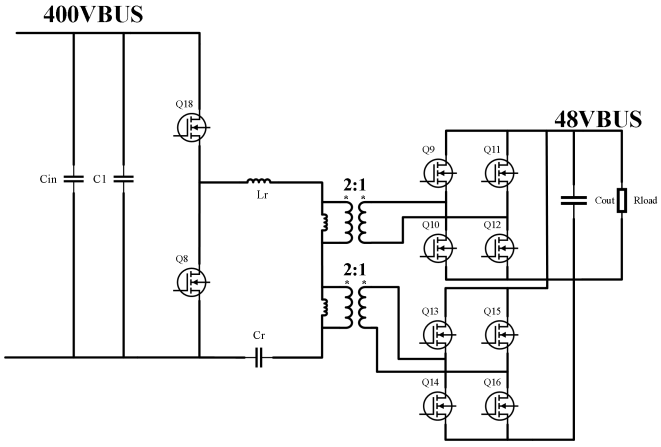

Fig. 2. LLC resonant converter with two-phase output

In order to reduce the transformer loss, we choose 300kHz as our resonant frequency. The auxiliary edge is parallel to two parties, which can be distributed on both sides to reduce the auxiliary copper loss. The primary side adopts a half bridge structure. For primary edge devices, the loss is mainly divided into conduction loss, shutdown loss and dead zone loss due to the implementation of ZVS. Comparing the corresponding device loss of the two schemes, two devices are used in

parallel in the half bridge, and four pipes are used in the full bridge. The loss of full bridge and half bridge is compared with the same number of pipes. The loss of half bridge is better than that of full bridge structure at 300k frequency.

At the same time, the half-bridge structure can reduce the transformer ratio and reduce the copper loss of the transformer winding. The overall turn ratio of the transformer is 4.

$$n = \frac{Vin}{2 \cdot Vout} \approx 4 \tag{1}$$

The winding structure adopts the structure of primary side in series and secondary side in parallel, and two units are used for parallel output. The primary side adopts a half bridge structure, and the turns ratio of each unit is 2:1.

A. Magnetic core structure design

For LLC operation mode of DCX, the output voltage is not modulated, so the gain curve can be designed to be very stable, the inductance ratio can be designed to be large, so the resonant inductance can be designed to be small. On the other hand, the excitation inductance is related to the size of the excitation current. The output capacitance of the switching device needs sufficient excitation current and deadtime to realize the ZVS of the primary side device. So the excitation inductance has a certain maximum value. The increase of excitation inductance is conducive to the reduction of magnetic loss. Therefore, if the excitation inductance meets ZVS, the magnetic loss can be reduced as much as possible. Through the derivation of the resonator loop, the excitation current I_m and dead time $t_{d\_\min}$ can be obtained:

$$I_m = \frac{nV_o}{4 f_s L_m} \tag{2}$$

$$t_{d\_\min} = \frac{2C_{oss}V_{in}}{I_m} \tag{3}$$

DMR95 is selected as the magnetic core material. In the application scenario below 500k, this material has lower specific loss compared with other materials. The following is the Steinmetz formula fitted according to the data in the material manual, and the unit of specific loss is W/m^3 :

$$P_v = 0.0014133 \cdot f^{2.04006} \cdot \Delta B^{2.72153} \tag{4}$$

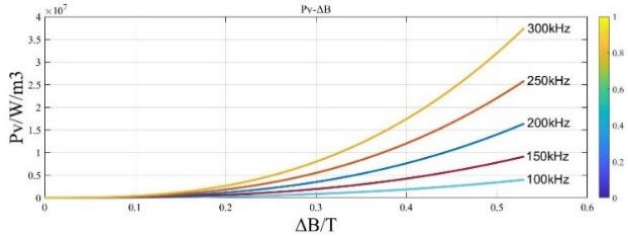

Fig. 3. The relationship of Bm and N

Consider the consumption of magnetic core loss and power density. The B_m is 100mt, so the size of the A_e required for the core of the magnetic core is:

$$Ae = \frac{nV_oT}{4B_mN_p} \tag{5}$$

For the selection of the shape of the center column, the winding design layout of the circular center column is not convenient for the square magnetic core. Meanwhile, the plate thickness The design of circular groove column can significantly reduce the hysteresis loss and eddy current loss in the core[1]. The optimization modeling is carried out for the middle column of the magnetic core, the winding width is assumed to be 3mm, the Ae value of the middle column has been determined, and the length and width of the slot need to be determined.

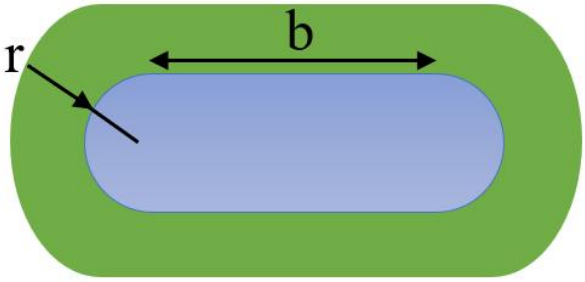

Fig. 4. Shape of center post and winding

The loss model of winding and magnetic core is established. Figure 5 shows the change of winding loss and magnetic core loss with the size of magnetic core. The optimization interval can be obtained and the size and shape of magnetic core can be finally determined,

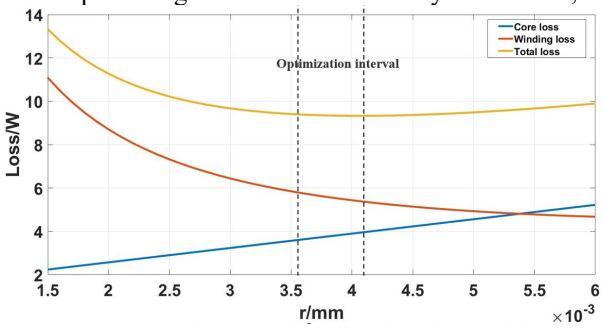

Fig. 5. Optimization of middle column loss model

The magnetic core structure integrates the transformer with the resonant inductor, and the inductor adopts EI type and matrix transformer integration. The purpose is to reduce the number of magnetic cores and the volume of magnetic cores.

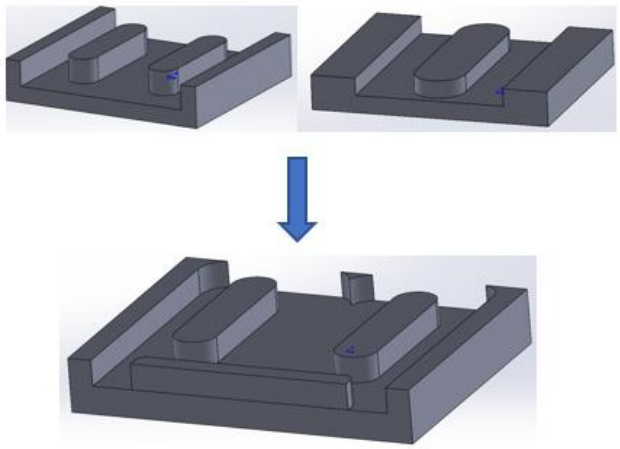

Fig. 6. Magnetic integration of inductance and transformer

The uniform distribution of magnetic flux density is conducive to reducing the uneven distribution of iron loss. If the magnetic flux loop of magnetic parts is analyzed, it can be found that if the magnetic flux of all side columns is half of that of the middle column, the reluctance ratio of side columns should be controlled:

$$\frac{2R_2+R_3+R_4}{2R_1+R_3+R_4}=\frac{3}{1} \tag{6}$$

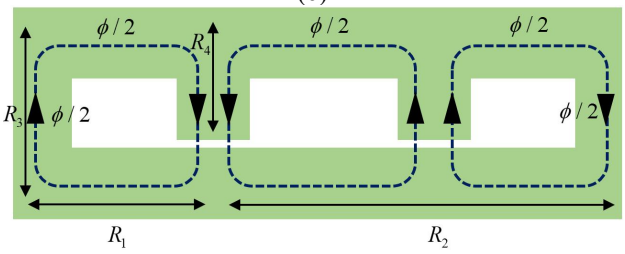

Fig. 7. Magnetic flux density distribution

To meet the formula(6), the magnetic flux of the border column can be kept uniform, which is conducive to reducing iron loss and improving the heat distribution of magnetic cores.

Therefore, the distance between the middle columns needs to be slightly larger than the distance between the side columns and the middle columns, so that the distribution of the magnetic flux density of the side columns can be uniform. The magnetic flux density of the core side cylinder can be evenly distributed by adjusting the distance of gap properly.

In fig.8, the left structure of core is called structure 1, and the right is called structure2. Compared with the structure 2, the structure 1 is convenient for the primary side PCB wiring, and only one turn is needed to obtain the required resonant inductance. For structure 2, the current density distribution of the winding at the column side of the resonant inductor is uneven. Structure 1 can reduce the uneven distribution of the current density of the winding, thus reducing the winding loss. However, since the middle column of the resonant inductor of structure 1 is larger than that of structure 2, this may lead to greater iron loss. Compared with the overall loss, the loss of structure 1 is lower.

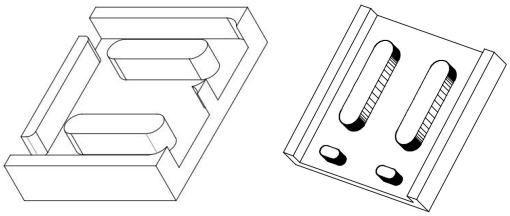

Fig. 8. Structure of magnetic(the left is structure1, and the left is structure2)

Through simulation comparison, the winding current density distribution of structure 1 is less uneven than that of structure 2, and the winding loss is lower. Although the magnetic core loss of structure 1 is larger, it is lower than the reduction rate of winding loss, and the overall loss of Structure 1 is well controlled.

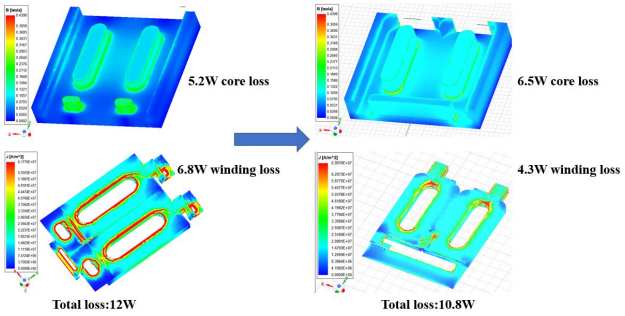

Fig. 9. Comparison of two structures loss

Through simulation of iron loss and copper loss, the total loss of structure 1 is 10.8W and that of structure 2 is 12W. After overall optimization, structure 1 has lower overall loss.

Under the designed parameters, the gain curve is stable. Figure 10 shows the gain curves at rated power, overload, and underload. The gain of the whole machine is nearly equal near the resonant frequency. In distributed power supply, open-loop control of the latter stage, the former stage PFC for bus voltage modulation.

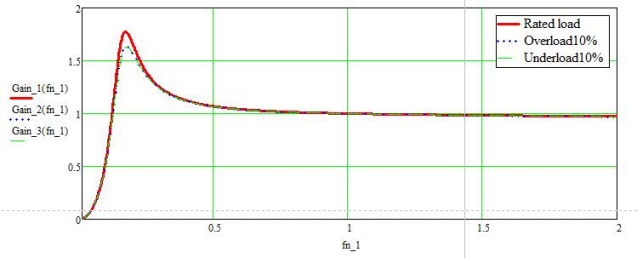

Fig. 10. Gain curve of LLC resonant converter with large Lm/Lr

B. *Winding structure design*

The winding adopts SPPS-SPPS structure, which has the lowest magnetomotive force between windings, and the distribution of magnetomotive force among windings is uniform, which can effectively reduce proximity effect and AC loss. The primary winding is wound on each central column for four turns, and the secondary winding is wound for two turns. The secondary winding is in a parallel two-layer structure. The first layer secondary side winding and the fifth layer secondary side winding are connected in parallel, and the fourth layer secondary side winding and the eighth layer secondary side winding are connected in parallel. The copper thickness is 3oz through loss comparison. As shown in Figure 5.

Fig. 11. The structure of windings

On the other hand, the parallel connection of the half-bridge pipe is compared with the non-parallel connection. By canceling the parallel connection, the whole shutdown loss of the switching device can be reduced, but the conduction loss will be increased. In fact, the ratio of device shutdown loss and conduction loss in

the overall switches loss is compared. Under the designed resonant frequency, the conduction loss accounts for a larger proportion, and the overall loss of the parallel device is lower than that of the non-parallel device. And figure 12 compare the efficiency of two situation. The peak efficiency of parallel is 0.6 higher than that of non-parallel.

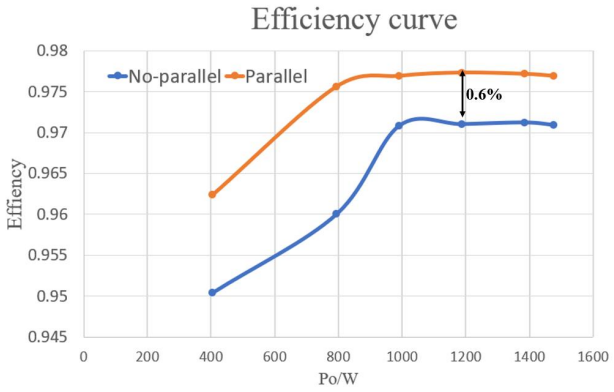

Fig. 12. Efficiency of parallel and no-parallel

At the same time, on the other hand, when the switching devices are reduced by half, Coss will be reduced, and the excitation inductance of the transformer can be further increased to reduce the magnetic loss, and the winding structure will change from the SPPS-SPPS to SPPS. At this time, the winding will reduce the degree of parallel connection, and the winding loss will increase. In order to verify the overall loss comparison between the two methods, finite element simulation and power device loss comparison were carried out. The design parameters of the two schemes are as Table I:

TABLE I
PARAMETERS OF TWO DESIGN

Table Head	Parameter	Parallel	No-Parallel	Unit
1	L_m	80	40	*uH*
2	N_{pri}	4	4	*turn*
3	$N_{\sec}$	2	2	*turn*
4	$C_{oss}@400V$	252	126	*pF*
5	Layer	8	4	/

Through the finite element simulation results, it can be found that the parallel structure has lower winding loss. Although the magnetic loss is larger than that of non-parallel structure, the copper loss is more different, so the total loss is larger. Figure 13 shows that core loss and winding loss of two winding structure. Parallel has lower total loss than no-parallel.

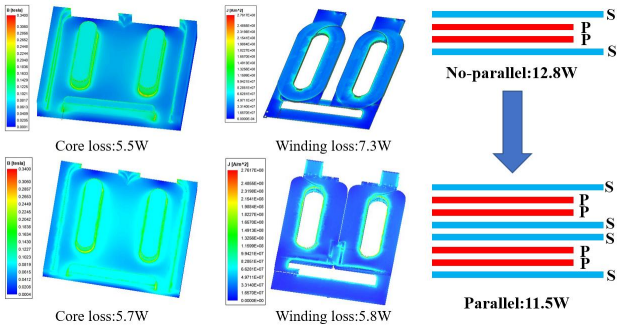

Fig. 13. Comparison of magnetic component loss

On the other hand, optimizing the position of the secondary side device can reduce the terminal loss of the secondary side device, thereby reducing the winding loss[1]. In this paper, the loop structure is optimized again. As shown in the figure 14， SR1 and SR4 are the switching devices of the turn-on path of the secondary side. The secondary winding current passes through SR1, then through the load, and back through SR4 to the transformer secondary side. The minimum terminal loop of this conduction path can achieve the optimal terminal loss.

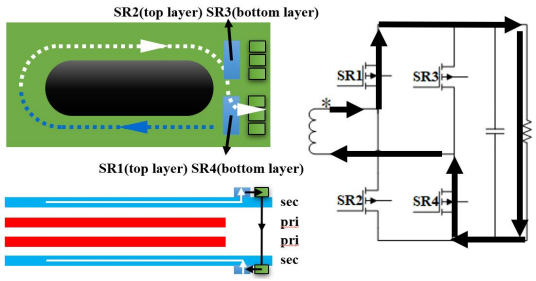

Fig. 14. LLC resonant converter with two-phase output

C. *Loss distribution*

With the development of the third generation wide band gap semiconductor, GaN devices have more excellent high frequency characteristics. By comparing the device characteristics of Infineon and GaN system, we can see that the FOM value of GaN is lower, and the lower the FOM value, the better the comprehensive performance of the device. The following table compares the performance of primary and secondary side devices.

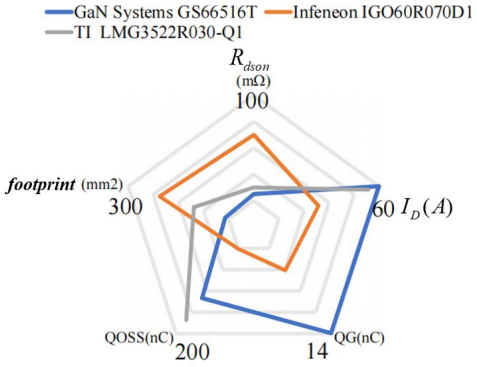

Fig. 15. Parameters of primary device

TABLE II
PARAMETERS OF SECONDARY DEVICE

Table Head	Parameter	EPC2033	EPC2021	IPB048N15N5	Unit
1	$V_{ds\max}$	150	80	150	*V*
2	$R_{ds(on)}$	7	2.2	4.8	*mΩ*
3	I_d	48	90	120	*A*
4	Q_g	12	15	80	*nC*
5	Q_{oss}	90	72	225	*nC*
6	V_{sd}	1.9	1.5	0.85	*V*
7	*FOM*	84	33	384	*pΩ*C*

Comparing MOS and GaN devices, we can see the advantages of GaN devices. Therefore, we choose

GS66516T as the primary LLC side device and EPC2021 as the secondary side device.

The loss of the whole machine includes the transformer loss, the conduction loss of the primary side device and the secondary side device, the shutdown loss and the drive loss. The loss of the whole machine is decomposed.

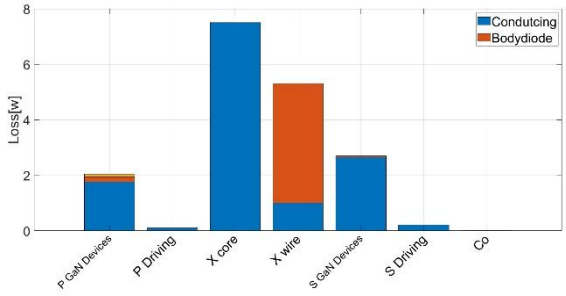

Fig. 16. Loss distribution of rated load

Through the loss decomposition of the whole machine, the loss of planar magnetic parts accounts for 50% of the total loss. At the same time, the half load condition is simulated and calculated, and the loss distribution at half load can be obtained. Estimated peak efficiency is 98.3%.

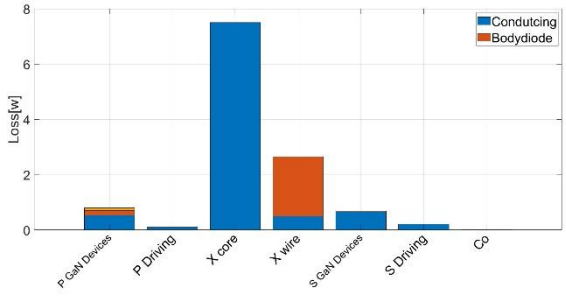

Fig. 17. Loss distribution of 50% rated load

III. Experiment Result

In this paper, two sets of prototypes are designed to test the actual efficiency and heat distribution. The table shows the test conditions. Finally, the two prototypes realized 390V DC input and 48V DC output. The parameters of experiment is listed in TABLE III:

TABLE III
Parameters of Experiment

Table Head	Parameter	Value	Unit
1	V_{in}	390	V
2	V_{out}	48	V
3	f_r	300	kHz
4	L_r	1	uH
5	L_m	40	uH
6	P_o	1500	W
7	PD	482(1)/488(2)	W/in^3
8	Primary Device	GS66516T	/
9	Secondary Device	EPC2021	/

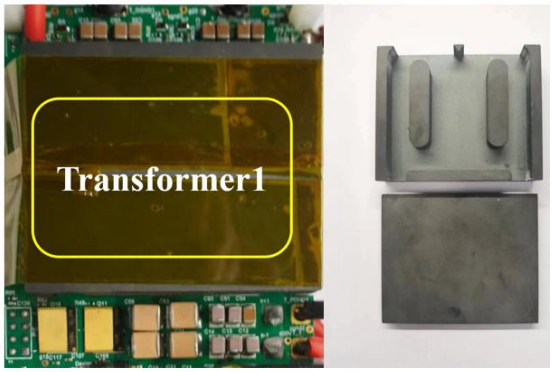

Fig. 18. Experiment board and magnetic core of structure1

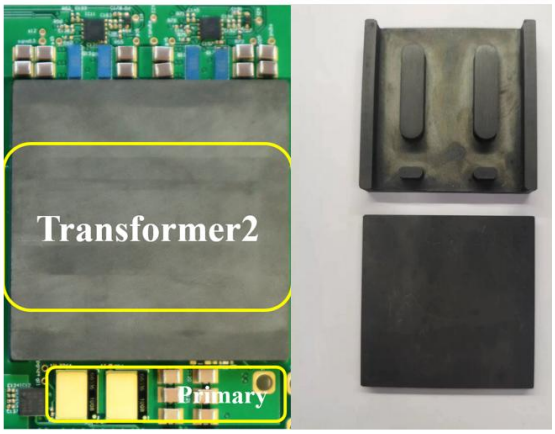

Fig. 19. Experiment board and magnetic core of structure2

For the test of efficiency curve, the input of the device is high voltage and the output is low voltage, so it is very important to accurately calibrate the input current and output voltage. Digital multimeter as input current detection and output voltage detection, so that we can get accurate efficiency curve. Figure 20 shows the experimental environment.

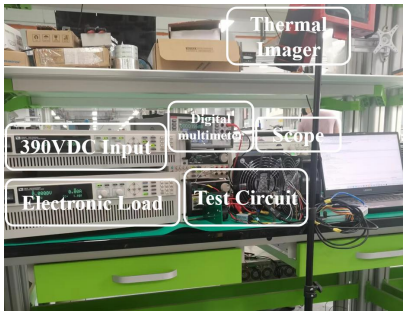

Fig. 20. Experiment environment

The whole machine has been tested, the input voltage is 390V, and the output voltage is 48V. The midpoint voltage and resonant current of the original and auxiliary bridge arms are tested. The dead time of the switching device is set to 150ns, which can realize the soft switching of the original side device.

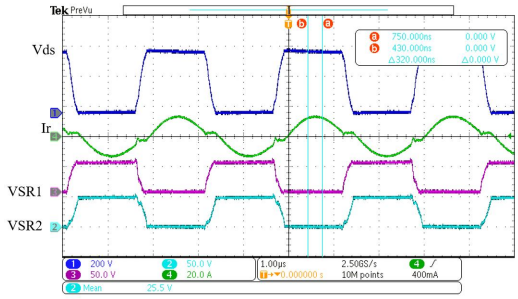

Fig. 21. The whole waveform of experiment

It can be seen from the test waveform that the primary side has achieved soft switching. In the test, a dot diode conduction time is reserved at the secondary side.

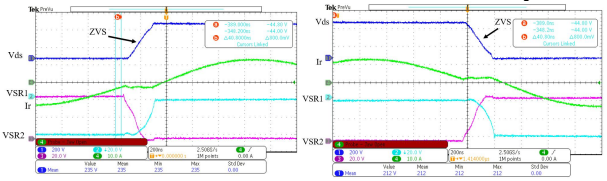

Fig. 22. Zero-switching waveform of primary device

The maximum temperature of the whole machine (structure1) is 46 ℃, of which the temperature of the original and secondary side power devices is 46 ℃, and the temperature of the magnetic core is 38 ℃.

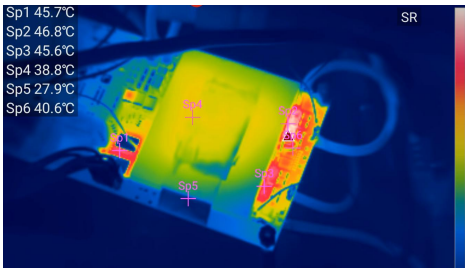

Fig. 23. Heat map of structure1

The figure shows the experimental heat distribution cloud diagram of Structure 2. Both the primary side and secondary side devices are at 50-60℃, the temperature of the magnetic parts is more than 50 ℃, and the temperature on the resonant inductor side of the transformer is as high as 65℃, and there is uneven heat distribution of the magnetic core.

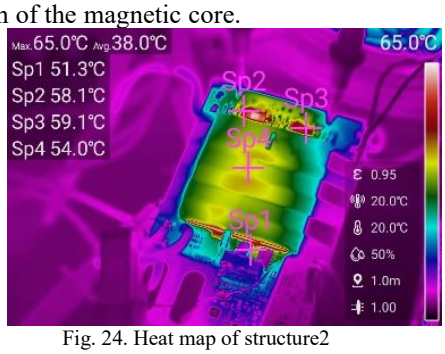

Fig. 24. Heat map of structure2

After secondary edge optimization, the temperature distribution of secondary edge is more uniform and the loss is smaller. And the temperature distribution of the core is more uniform.

In the experiment, high-precision multimeter is used to accurately measure the input and output parameters to obtain accurate efficiency curves. It can be seen from the efficiency curve that the efficiency of the two prototypes is similar when they are under heavy load, and the efficiency of structure 1 is higher when they are under light load. The peak efficiency of the whole machine is 97.8%, and the full load efficiency is 97.6%.

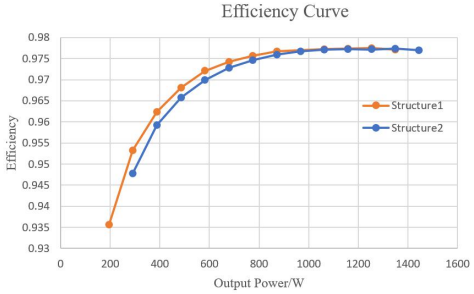

Fig. 25. Efficiency of two structure

IV. Conclusions

In this paper, the winding structure is optimized, and the magnetic column on the resonant inductor side is optimized, which makes the PCB winding structure simpler and the winding loss lower. At the same time, the position of the secondary side device is optimized to reduce the terminal loss of the secondary side winding. Finally, the prototype achieves 97.8% peak efficiency and 97.6% full load efficiency. And power density of the whole machine is 488 W/in^3. And the optimized core heat distribution is more uniform.

Acknowledgment

Thanks to UNISOC for their support for communication power projects.

References

[1] R. Gadelrab, A. Nabih, F. C. Lee and Q. Li, "LLC Resonant Converter with 99% Efficiency for Data Center Server," 2021 IEEE Applied Power Electronics Conference and Exposition (APEC), 2021, pp. 310-319, doi: 10.1109/APEC42165.2021.9487423.

[2] Bo Yang, F. C. Lee, A. J. Zhang and Guisong Huang, "LLC resonant converter for front end DC/DC conversion," APEC. Seventeenth Annual IEEE Applied Power Electronics Conference and Exposition (Cat. No.02CH37335), Dallas, TX, USA, 2002, pp. 1108-1112 vol.2, doi: 10.1109/APEC.2002.989382.

[3] D. Fu, B. Lu and F. C. Lee, "1MHz High Efficiency LLC Resonant Converters with Synchronous Rectifier," 2007 IEEE Power Electronics Specialists Conference, Orlando, FL, USA, 2007, pp. 2404-2410, doi: 10.1109/PESC.2007.4342388.

[4] Bo Yang, Rengang Chen and F. C. Lee, "Integrated magnetic for LLC resonant converter," APEC. Seventeenth Annual IEEE Applied Power Electronics Conference and Exposition (Cat. No.02CH37335), Dallas, TX, USA, 2002, pp. 346-351 vol.1, doi: 10.1109/APEC.2002.989269.

[5] D. Huang, S. Ji and F. C. Lee, "LLC Resonant Converter With Matrix Transformer," in IEEE Transactions on Power Electronics, vol.29,no.8,pp.43394347,Aug.2014,doi:10.1109/TPEL.2013.2292676.

[6] A. Nabih, R. Gadelrab, P. R. Prakash, Q. Li and F. C. Lee, "High Power Density 1 MHz 3 kW 400 V-48 V LLC Converter for Datacenters with improved Core Loss and Termination Loss," 2021 IEEE Applied Power Electronics Conference and Exposition (APEC),2021,pp.304-309,doi:10.1109/APEC42165.2021.9487232.